ELSEVIER

Biochimica et Biophysica Acta 1369 (1998) 287–294

BIOCHIMICA ET BIOPHYSICA ACTA
BBA

Relationship between polypeptide transcytosis and lymphoid tissue in the rabbit nasal mucosa

Dario Cremaschi *, Roberta Ghirardelli, Cristina Porta

Dipartimento di Fisiologia e Biochimica Generali (Sezione di Fisiologia Generale), Università degli Studi di Milano, Via Celoria 26, I-20133 Milan, Italy

Received 29 July 1997; revised 19 September 1997; accepted 24 September 1997

Abstract

It has been suggested that the specific transcytosis of polypeptides, demonstrated in rabbit nasal mucosa (upper concha), is involved in antigen sampling at the airway entry. To test this hypothesis, unidirectional transepithelial fluxes of carbocalcitonin (CCT Mw = 3362) from the mucosal to the submucosal side, and vice versa, were measured by radioimmunoassay every 30 min for 120 min and, from the difference, net absorption was determined in the upper concha and septum mucosae. The exposed mucosae were examined by quantitative histology; isolated scattered lymphoid cells/mm^2 and volumes of lymphoid infiltrates and aggregates were quantified. CCT absorption was observed in the mucosae of the upper concha and septum provided that aggregates were present, being proportional to aggregate volume. No relationship was noted with isolated scattered lymphoid cells and infiltrates. Passive permeability was unaffected by lymphoid tissue. On this basis, the antigen sampling hypothesis seems to be at least partially substantiated. © 1998 Elsevier Science B.V.

Keywords: Active transport of polypeptides; Lymphoid aggregate; Antigen sampling; Upper concha; Septum

1. Introduction

Specific transcytosis of polypeptides has been demonstrated in rabbit nasal mucosa, in the region of the upper concha [1–3].

The nasal localization of the transport and its small entity and transient duration suggested that the function involved was not to massively absorb material but to transfer chemical messages from nasal lumen to blood; in particular, as the transport relates to polypeptides, it might be involved in antigen sampling from the lumen at the entry of the airways [1,2,4].

Similar antigen sampling stations have been found along the bronchi [5–10] and, primarily, in intestinal Peyer's patches [9], where the epithelium – containing antigen sampling cells – lies on lymphoid tissue, to which the antigens transported across the mucosa are addressed; thus, a defensive immunological response against potential noxious material present in the airway or intestinal lumen can be developed before this material crosses the epithelium massively.

Intra- and sub-epithelial lymphoid cells have been observed in nasal mucosa. The latter are more or less

* Corresponding author. Fax: +39-2-70644702; E-mail: daricrem@imiucca.csi.unimi.it

PII S0005-2736(97)00232-0

scattered, even gathered in thick infiltrations [11–13], and in the case of dog and rat also organized in aggregates and follicle-like aggregates [12,14,15]. In particular, circular lymphoid masses, 300–450 μm in diameter, covered by an epithelium consisting mainly of non-ciliated microvillar cells, have been noted in the upper concha of the rabbit [16].

Our first histological inspection of the upper concha subepithelial tissue in the rabbit showed that the extent and organization of lymphoid tissue were somewhat variable; likewise polypeptide transcytosis proved very similar in some animal groups but highly variable in others [1,2]. On this basis, in order to examine whether the transcytosis observed serves the lymphoid tissue as it is being involved in antigen sampling, we studied whether any quantifiable relationship occurs between extent of transport and lymphoid tissue.

2. Materials and methods

Male New Zealand rabbits weighing ≈ 3 kg were killed by cervical dislocation and the nasal mucosae from the roof or the septum of both nostrils were mechanically excised very carefully, washed with Krebs–Henseleit saline at room temperature and mounted on frames between two Teflon chambers. The exposed part of the mucosa (area: 0.3 cm^2) corresponded to that covering the upper nasal concha or the central septum. The two chambers were filled with 1 ml Krebs–Henseleit saline, bubbled with prehumidified 95% O_2 + 5% CO_2 to oxygenate the tissue, maintain the pH at 7.4 and agitate the solution. The experiments were carried out at a monitored temperature of 27 ± 1°C: at this temperature, the transports were half those measured at 37°C, but the isolated mucosa was stable and viable for hours and the peptide was much more stable with respect to time [17].

2.1. Transepithelial electrical potential difference and flux measurements

The transepithelial electrical potential differences (V_{ms}) were measured, as previously reported [1,17], to check the viability of the epithelium at the beginning, during and at the end of the experiment.

Flux measurements were also carried out on the test molecule (elcatonin or carbocalcitonin (CCT): [1,7 Asu]eel calcitonin; Mw = 3362) as previously reported [1]. Briefly, the mucosa-submucosa unidirectional flux (J_{ms}) and the reversed flux (J_{sm}) were determined (one on the right, the other on the left mucosa from the same animal) with random combinations, the functional symmetry of the two mucosae being known [1,17]. After a 30 min preincubation to allow the tissue to recover after isolation, 1 ml saline with 20 μg/ml CCT was introduced into the mucosal or submucosal chamber (donor saline) and the corresponding transepithelial flux was subsequently determined by complete withdrawal and immediate replacement of the saline (1 ml). J_{ms} and J_{sm}, each measured every 30 min for 120 min, were considered unidirectional, since the maximal concentration reached in the flux chamber was 10^{-3}–10^{-5} of the concentration in the donor saline. CCT monitoring in the donor saline and flux corrections were as previously reported [1,2]. CCT was determined by radioimmunoassay (RIA) so as to measure only the intact or nearly intact molecule [1,3].

2.2. Histological preparations and measurements

After the flux measurements the exposed mucosae (3 × 10 mm well delimited by the scratch left by the frame pressure) were cut away and fixed in Bouin saline, embedded in paraffin and cut into 8 μm thick sections, regularly taken every 67 μm, along the main axis (10 mm) of the piece of mucosa. All sections were then stained with hematoxylin–eosin. With a 320–400 × magnification, and with the aid of an eye-piece fitted with a calibrated reticulum, all sections were examined to observe the isolated lymphoid cells, scattered in the mucosal layer just beneath the epithelium (50 μm thick layer), and in addition lymphoid infiltrates and aggregates distributed on all the tissue thickness. Lymphoid cells were morphologically identified. To calculate the apparent number of the isolated scattered lymphoid cells/mm^2, the scattered lymphoid cells observed in all sections were totalled and the total divided by the tissue surface area (0.3 cm^2). The approximate mean actual number

of the isolated scattered lymphoid cells/mm^2 was equal to the apparent number/mm^2, multiplied by 8.4 (hypothetical number of sections in the 67 μm). Lymphoid infiltrates appeared approximately similar to cylindroids: thus, to calculate their volume (V), they were considered cylindroids whose two axes a and b were measured in the section and length l measured by the number of sections in which that infiltrate appeared, multiplied by 67 μm ($V = \pi abl$). Lymphoid aggregates appeared approximately similar to spheres ($V = \frac{4}{3}\pi a^3$) or ellipsoids (two axes were measured in the central section, the third half the number of sections in which that aggregate appeared, multiplied by 67 μm, $V = \frac{4}{3}\pi abc$). The morphological distinction between infiltrates and aggregates is reported in Section 3.

2.3. Bathing salines

The Krebs–Henseleit solution had the following composition (mM): 142.9 Na^+, 5.9 K^+, 2.5 Ca^{2+}, 1.2 Mg^{2+}, 127.7 Cl^-, 24.9 HCO_3^-, 1.2 SO_4^{2-}, 1.2 $H_2PO_4^-$, 5.5 glucose; pH 7.4. Cytochalasin B was dissolved in ethanol and added with it to the Krebs–Henseleit saline (2.5 μl ethanol/ml) to reach a final concentration of 10 μg cytochalasin B/ml (21 μM) [2]. Aluminum fluoride (AlF_4^-, 100 μM) was prepared as previously described [2]. The inhibitors were added on both sides and remained in the media throughout the experiment (i.e. during the 30 min preincubation and the 120 min incubation periods).

2.4. Materials

Elcatonin and its antibody for RIA were supplied by ISF-Biomedical Research Laboratories (Trezzano sul Naviglio, Milan, Italy), where RIA for elcatonin has been set up [2]. Cytochalasin B, $Al_2(SO_4)_3$ and KF were supplied by Sigma (St. Louis, MO).

2.5. Statistics

When results are expressed as means ± standard errors, Student's t-test for unpaired or, when possible, for paired data was used for statistical analysis. Straight lines were calculated by the linear regression method.

3. Results

3.1. Histological observations

The mucosa covering the upper concha (335 ± 10 μm thick, $n = 10$) proved to be rich in capillaries and well-delimited by two parallel, longitudinal vessels; its respiratory epithelium was 78.0 ± 1.6 μm thick ($n = 10$). The septum tissue was significantly thicker (440 ± 35 μm, $n = 10$, $p < 0.01$) and contained fewer vessels; its respiratory epithelium was thinner (63.6 ± 5.5 μm, $n = 10$, $p < 0.05$). In both, upper concha and septum, part of the mucosa was rich in glands (gm) and part scarsely glandular (sgm); gm was occupied by glands for ~80% and sgm for ~6%. However, septum mucosa was much more abundant in gm than concha (>80%, $n = 30$ vs. ~45%, $n = 22$) so that the total space occupied by glands in septum mucosa was ~70% ($n = 30$) against ~40% ($n = 22$) in concha (see Fig. 1(a) and (b)).

Lymphoid tissue was present in both, concha and septum mucosae. Isolated scattered lymphoid cells were observed; sometimes lymphoid cells were gathered into poorly delimited, diffuse lymphoid infiltrates, penetrated by many glands (Fig. 1(c)). The infiltrates displayed variable dimensions and could approximately be compared with cylindroids; thus, their volume could be calculated (see Section 2) and then corrected for the space occupied by glands. The lymphoid tissue also appeared as thick lymphoid cell aggregates, not penetrated by glands. Some aggregates were very small, without defined organization, but very well delimited; others were larger, less delimited, without clear organization, extending into the epithelium (Fig. 1(d)); a third type displayed a minimum of organization (differentiated central region, corona), in some ways similar to that of intestinal Peyer's patch follicles, but not so well defined (Fig. 1(e)). All aggregates could be approximately compared to spheres or ellipsoids and their volume so calculated (see Section 2). The mucosa covering the upper concha appeared to contain more lymphoid

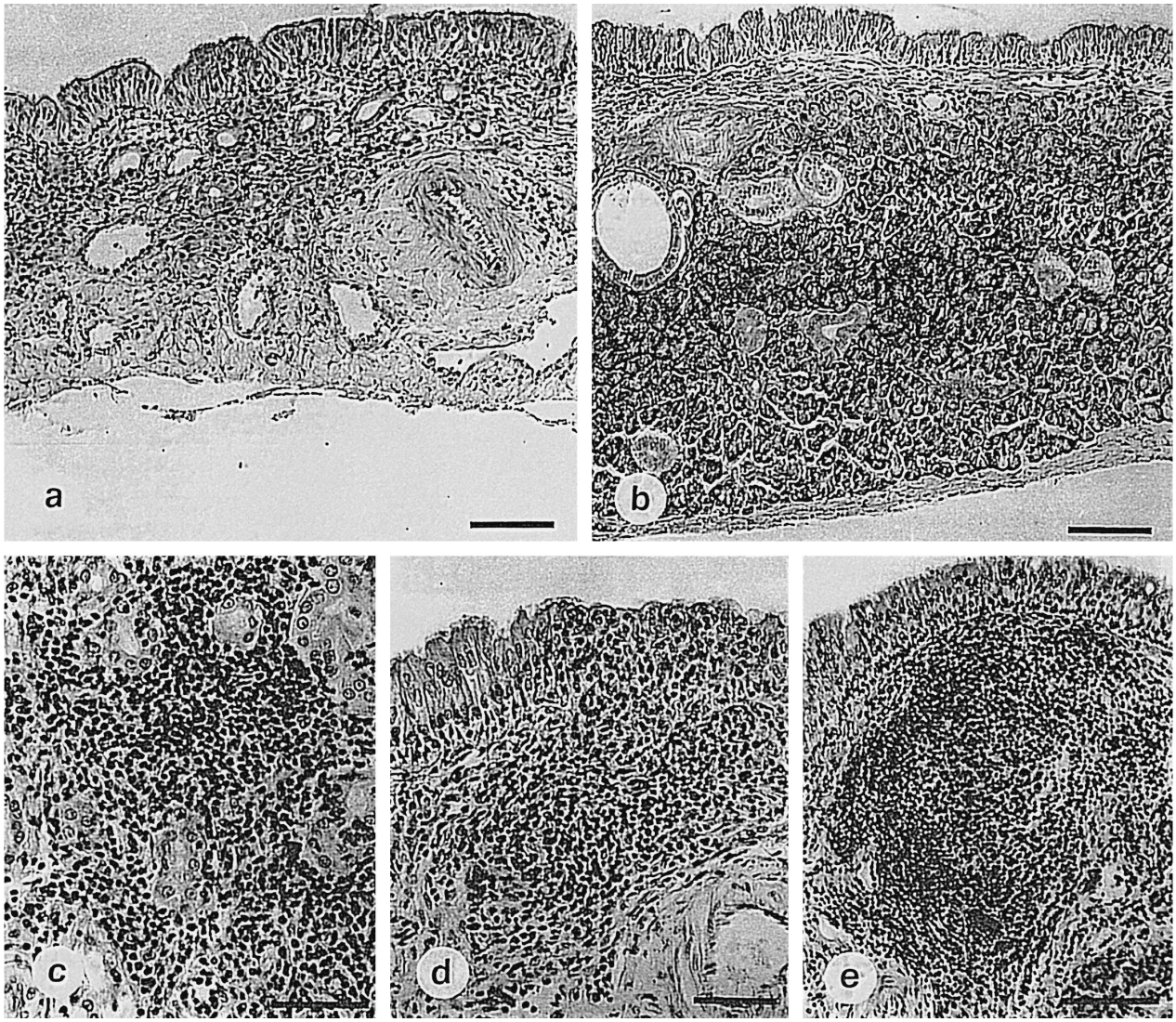

Fig. 1. Sections of the mucosa covering (a) – the upper concha and (b) – septum: the much larger percentage of glands in the septum is evident. (c) – Isolated scattered lymphocytes and lymphoid infiltrates diffused among the glands are observed. Lymphoid aggregates are thick, more delimited and not penetrated by glands; they sometimes prove to be very small, well-delimited, but without defined organization; (d) – sometimes are larger, not so well-delimited, without definite organization and clearly extending themselves into the epithelium; and (e) – in some cases, aggregates tend to have a minimal organization with a central region and a corona, somewhat like follicles of intestinal Peyer's patches, but not so well-defined. The bars in (a), (b) and (e) correspond to 100 μm, and those in (c) and d) to 50 μm. Magnifications are: 125 × for (a) and (b), 290 × for (c), 250 × for (d), and 145 × for (e).

tissue (infiltrates and aggregates) than that covering the septum ($987.10^3\,\mu m^3$ lymphoid tissue/mm^2 mucosa, $n = 22$, against $337.10^3\,\mu m^3/mm^2$, $n = 30$); taking account of the volume of lymphoid aggregates alone, it seemed to be larger in the mucosa of the upper concha (175.10^3 vs. $101.10^3\,\mu m^3/mm^2$). Finally, individual tissues taken from either upper concha or septum, displayed different contents of isolated scattered lymphoid cells, infiltrates and aggregates and different predominance ratios.

3.2. Upper concha: CCT active / passive fluxes and lymphoid tissue

The carbocalcitonin (CCT) net absorptions, displayed by the mucosae facing the upper concha, were

highly variable. On the basis of this observation, 11 paired mucosae were fixed at the end of CCT flux measurements and prepared for histological analysis as described in Section 2. The flux time-course was similar to that previously observed and is not reported here for the sake of brevity: the passive submucosa–mucosa unidirectional flux (J_{sm}) was stable throughout the experiment, whereas the mucosa–submucosa unidirectional flux (J_{ms}) and the corresponding net flux (J_{net}) had a maximal value during the first 30 min measurement period, then gradually declined.

The relationship between maximal CCT net absorption and content of lymphoid tissue in each of the 11 mucosae on which (J_{ms}) had been measured was then examined. No relationship was shown to exist between transport and isolated lymphoid cells scattered in the layer of mucosa just beneath the epithelium (50 μm thick layer), nor between transport and volume of all lymphoid infiltrates (former case: $r = 0.4277$, $n = 12$, n.s.; latter case: $r = 0.4769$, $n = 11$, n.s.). Conversely Fig. 2(a) shows that, a linear, positive relationship exists between transport (y) and volume of all lymphoid aggregates (x). The interpolating straight line can be expressed by the equation:

$$y = (2.5 \pm 1.8) + (11.0 \pm 1.3) \times 10^{-6} x \qquad (1)$$

Since the intercept with the y-axis is not significantly different from zero, CCT net absorption only seems to appear on condition that aggregates are present and increases with their volume. It is to emphasize that the total aggregate volume included all the three forms of aggregates described above.

Fig. 2(b) shows that, in parallel, the passive unidirectional flux (J_{sm}) of CCT (and, as a consequence, passive permeability) is independent of aggregate presence, as the flux is relatively small (1.4–5.8 ng cm^{-2} h^{-1}) even in the presence of very large volumes of aggregates.

As a countercheck, the observations were extended to mucosae whose net absorption was abolished by treatment with inhibitors of vesicular transports (e.g. AlF_4^- and cytochalasin B, see Ref. 2): net absorption was nil, in spite of the presence of lymphoid aggregates in the mucosae. This was shown by the histological analysis performed on seven tissues treated with 100 μM AlF_4^- and four tissues treated with 21 μM cytochalasin B. The maximal net absorptions of CCT and volumes of lymphoid aggregates for each mucosa are reported in Fig. 2(c) in which, for the purpose of comparison, the dashed line represents the relationship under control conditions (straight line calculated from Fig. 2(a) and Eq. (1)).

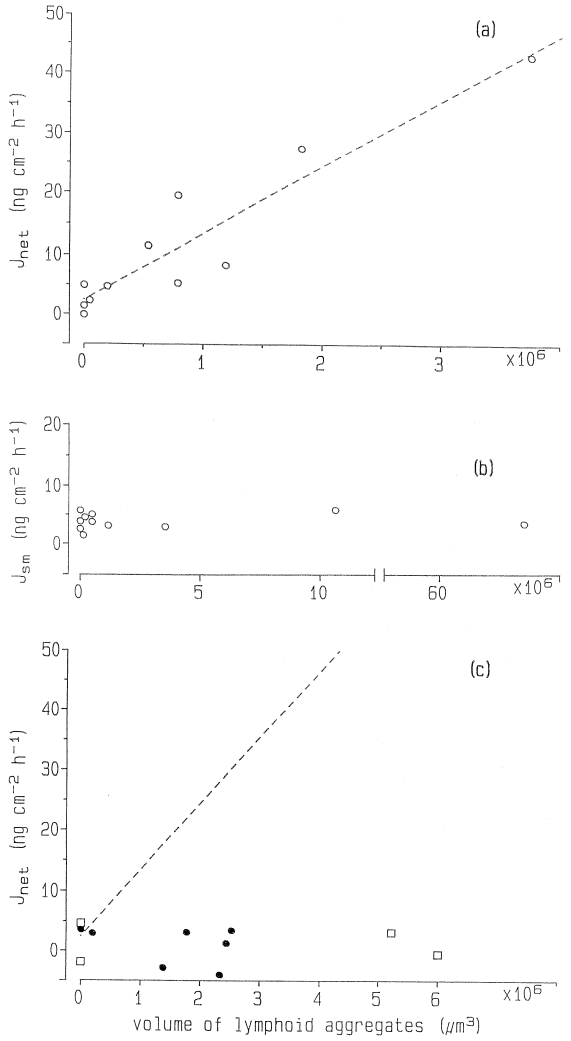

Fig. 2. Upper concha: relationship between carbocalcitonin (CCT) fluxes and volume of all lymphoid aggregates: (a) – maximal net absorption of CCT vs. volume of lymphoid aggregates (straight line: $r = 0.9400$, $n = 11$, $p < 0.01$); (b) – passive permeability (indexed by unidirectional submucosa–mucosa flux of CCT, J_{sm}) vs. volume of lymphoid aggregates; and (c) – maximal net absorption of CCT, under treatment with 100 μM AlF_4^- (•) or 21 μM cytochalasin B (□) vs. volume of lymphoid aggregates (the dashed line represents the straight line calculated in Fig. 2(a) under control conditions; shown for comparison).

3.3. Septum: CCT active / passive fluxes and lymphoid tissue

Only the upper concha mucosa had shown an active polypeptide absorption among the respiratory mucosae covering the three different nasal regions previously studied (ectoturbinal A, lower and upper concha, Ref. [2]). We can now show that septum mucosa also is able to absorb. Of the six paired septal mucosae, two had net absorption close to zero (as a mean in $ng\,cm^{-2}\,h^{-1}$: $J_{ms} = 2.6$, $J_{sm} = 1.1$, $J_{net} = 1.5$), but four had a significant net absorption. J_{sm} was small and stable over time ($2.4 \pm 0.9\,ng\,cm^{-2}\,h^{-1}$); J_{ms} was high during the first 30 min period ($62.7 \pm 16.7\,ng\,cm^{-2}\,h^{-1}$), but then gradually declined with a time course similar to that observed for J_{ms} measured across the upper concha mucosa. Correspondingly, J_{net} was initially $60.2 \pm 17.2\,ng\,cm^{-2}\,h^{-1}$ and then declined. The high standard errors reported emphasize a large absorption variability.

On the basis of the histological analysis carried out on these six septum mucosae no relationship was observed between maximal net transport and the number of isolated lymphoid cells scattered in the layer just underlying the epithelium, or between maximal net transport and the volume of all lymphoid infiltrates (correlation coefficient: not significant in both cases). On the contrary, as for the upper concha mucosae, a linear, positive correlation was shown between maximal net transport (y) and volume of all lymphoid aggregates (x) (Fig. 3(a)), the interpolating straight line being expressed by the equation:

$$y = (3.1 \pm 1.6) + (14.1 \pm 0.5) \times 10^{-6} x \qquad (2)$$

The straight line intercept with the y-axis is not different from zero; thus, net CCT absorption again seems to appear only if aggregates are present and to increase with their volume; moreover, the slope of Eq. (2) is not significantly different from the slope of Eq. (1). It is worth noting that the total aggregate volume was comprehensive of all the three forms of aggregates described above.

Passive permeability (indexed by J_{sm}) proved to be independent of the volume of the lymphoid aggregates (Fig. 3(b)).

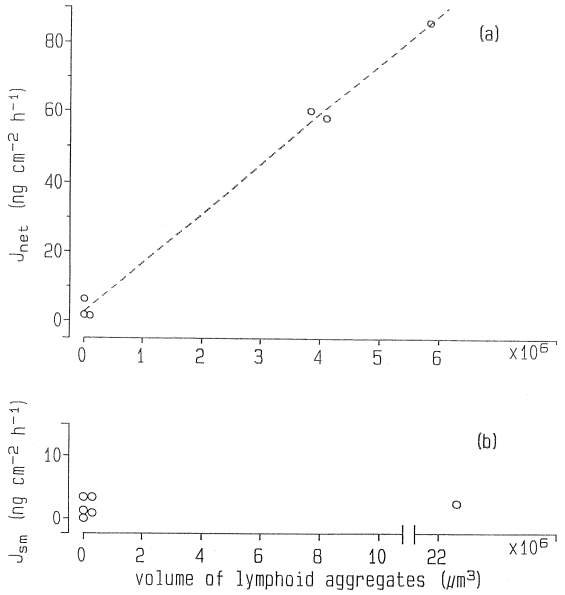

Fig. 3. Septum: relationship between carbocalcitonin (CCT) fluxes and volume of all lymphoid aggregates. (a) – Maximal net absorption of CCT vs. volume of lymphoid aggregates (straight line: $r = 0.9976$, $n = 6$, $p < 0.01$); and (b) passive permeability (indexed by J_{sm}) vs. volume of lymphoid aggregates.

4. Discussion

Previous work has shown that in the mucosa covering the nasal upper concha a specific, metabolic-dependent, net absorption of polypeptides, with saturation kinetics, transient duration and low transport capacity, occurs; since it can be abolished by inhibitors of vesicular transport and receptor-mediated endocytosis and can also take place with polypeptides adsorbed on latex nanospheres, it appears to be an active and specific transcytosis with the likely end to carry short pulses of chemical messages [1–4].

The main observation of this paper is that this active and specific polypeptide transcytosis is correlated with the volume of lymphoid aggregates present in the mucosa. Besides, in the upper concha this transport has not previously been observed in other nasal regions such as the lower concha and ectoturbinal A [2]; however, it has now been demonstrated that the septum region can also develop it, although with a high absorption variability, which requires further observations to better define its mean extent. In the septum too, the absorption is correlated

to the volume of lymphoid aggregates. The correlation is linear and positive for both upper concha and septum. The two calculated straight lines, which express the correlation, cross the origin and their slopes are not significantly different from each other, in spite of the fact that the two tissues have different features: the septum mucosa is thicker, with thinner epithelium, less vascularized, much richer in glands and poorer in lymphoid tissue, in general, and lymphoid aggregates in particular. This strengthens the connection between absorption and volume of lymphoid aggregates even more. Conversely, passive permeability, indexed by J_{sm}, is independent of lymphoid aggregate volume both in upper concha and septum mucosa.

To sum up, the net absorption seems to serve lymphoid cells organized in aggregates. In fact:

1. absorption only occurs on condition that aggregates are present;
2. the larger the volume of aggregates to be served, the larger is the absorption;
3. no relationship exists with less organized lymphoid tissue (isolated scattered lymphoid cells, simple diffuse infiltrates).

In Peyer's patches of the small intestine, polypeptide transcytosis also serves organized lymphoid tissue, although the level of organization of lymphoid tissue in that case is higher [9]. On the basis of these observations, the hypothesis that this transport represents antigen sampling from the nose lumen is more strengthened.

Transport is likely to be regulated by a complex control mechanism which, however, on the basis of the present results, seems to be set up primarily by activating messages sent from lymphoid aggregates. Interactions between epithelia and lymphoid tissue are well known. Epithelial cells themselves can produce cytokines that control epithelial and subepithelial cell proliferation and differentiation [18]; moreover, epithelial cells specialized in transporting antigens subepithelially in this way affect macrophages, T helper cells, dendritic cell and finally B lymphocytes, with production cascade step-by-step of cytokines, carrying different messages which lead to a final immunological response [9,19,20]. Messages sent by the epithelial cells to lymphoid tissue, thus, generate the production of new messages which go back from the lymphoid tissue to the epithelial cells, activating Cl^- and water secretion for example (for a short review, see Ref. [21]). Among the various types of polypeptide transport, secretion of polymeric immunoglobulin A (pIgA) is certainly under the control of gamma interferon (IFN-γ), which is produced by activated T cells; IFN-γ enhances the expression of secretory component (SC), which is the receptor for pIgA, present on the basolateral membrane of some epithelial cells (crypt cells, exocrine glandular tissues), and facilitates the transport of these immunoglobulins through the epithelial cells into exocrine fluids [20,22].

Acknowledgements

We are indebted to Dr. F. Bonasoro for photographs of histological preparations, and to Dr C. Rizzi for her valuable help in histological analysis.

References

[1] D. Cremaschi, C. Rossetti, M.T. Draghetti, C. Manzoni, V. Aliverti, Active transport of polypeptides in rabbit nasal mucosa: Possible role in the sampling of potential antigens, Pflügers Arch. 419 (1991) 425–432.

[2] D. Cremaschi, C. Porta, R. Ghirardelli, C. Manzoni, I. Caremi, Endocytosis inhibitors abolish the active transport of polypeptides in the mucosa of the nasal upper concha of the rabbit, Biochim. Biophys. Acta 1280 (1996) 27–33.

[3] D. Cremaschi, C. Porta, R. Ghirardelli, The active transport of polypeptides in the rabbit nasal mucosa is supported by a specific vesicular transport inhibited by cytochalasin D, Biochim. Biophys. Acta 1283 (1996) 101–105.

[4] D. Cremaschi, C. Porta, R. Ghirardelli, Endocytosis of polypeptides in the nasal respiratory mucosa of the rabbit, News in Physiol. Sci. (1997) in press.

[5] J.T. Richardson, T. Bouchard, C.C. Ferguson, Uptake and transport of exogenous proteins by respiratory epithelium, Lab. Invest. 35 (1976) 307–314.

[6] R.P. Michel, S. Inoue, J.C. Hogg, Pulmonary capillary permeability to HRP in dogs: A physiologic and morphologic study, J. Appl. Physiol. 42 (1977) 13–21.

[7] K. Tenner-Racz, P. Racz, K.N. Myrvik, J.R. Ockers, R. Geister, Uptake and transport of horseradish peroxidase by lymphoepithelium of the bronchus-associated lymphoid tissue in normal and bacillus Calmette–Guérin immunized and challenged rabbits, Lab. Invest. 41 (1979) 106–115.

[8] M.R. McDermott, A.D. Befus, J. Bienenstock, The structural basis for immunity in the respiratory tract, Int. Rev. Exp. Pathol. 23 (1982) 47–112.

[9] R.L. Owen, Ultrastructure of antigen trapping epithelia of mucosal lymphoid organs, in: Mucosal Immunoregulatory Mechanisms, 8th Int. Convoc. Immunol., Amherst, New York, 1982; Basel, Karger, 1983, pp. 88–98.
[10] L.G. Johnson, P.W. Cheng, R.C. Boucher, Albumin absorption by canine bronchial epithelium, J. Appl. Physiol. 66 (1989) 2772–2777.
[11] S. Katz, J. Merrel, Distribution of epithelia and glands of the nasal septum mucosa in the rat, Acta Anat. 99 (1977) 58–66.
[12] D.R. Adams, D.K. Hotchkiss, The canine nasal mucosa, Anat. Histol. Embryol. 12 (1983) 109–125.
[13] D.R. Adams, Transitional epithelial zone of the bovine nasal mucosa, Am. J. Anat. 176 (1986) 159–170.
[14] D.M.H. Hameleers, M. Van der Ende, J. Biewenga, T. Sminia, An immunohistochemical study on the postnatal development of rat nasal-associated lymphoid tissue (NALT), Cell Tissue Res. 256 (1989) 431–438.
[15] B.J. Spit, E.G.J. Hendriksen, J.P. Bruijntjes, C.F. Kuper, Nasal lymphoid tissue in the rat, Cell Tissue Res. 255 (1989) 193–198.
[16] A. Shimamura, H. Toh, Scanning electron microscopic observations of the nasal mucosa in the rabbit, J. Electronmicrosc. 23 (1974) 277.
[17] D. Cremaschi, C. Rossetti, M.T. Draghetti, C. Manzoni, C. Porta, V. Aliverti, Transepithelial electrophysiological parameters in rabbit respiratory nasal mucosa isolated in vitro, Comp. Biochem. Physiol. 99A (1991) 361–364.
[18] A.W. Stadnyk, Cytokine production by epithelial cells, FASEB J. 8 (1994) 1041–1047.
[19] T. Kato, R.L. Owen, Structure and function of intestinal mucosal epithelium, in: Handbook of Mucosal Immunology, Academic Press Inc., S. Diego, 1994, pp. 11–26.
[20] H. Kiyono, J.R. McGhee, T helper cells for mucosal immune responses, in: Handbook of Mucosal Immunology, Academic Press Inc., S. Diego, 1994, pp. 263–274.
[21] G.A. Castro, Gut immunophysiology: Regulatory pathways within a common mucosal immune system, News in Physiol. Sci. 4 (1989) 59–64.
[22] L.M. Sollid, P. Brandtzaeg, D. Kvale, G. Gaudernack, H. Scott, E. Thorsby, T cell–epithelium interactions in relation to gut immunity, in: Monographs in Allergy, P. Dukor, L.A. Hanson, P. Kallós, F. Shakib, Z. Trnka, B.H. Waksman (Eds.), Karger, Basel, 1988, vol. 24, pp. 60–65.